

experimental measurements that confirm a precision of 8 bits down to 19.6pA.

II. ‘Stochastic I-Pot’ Circuit Description

The ‘Stochastic I-Pot’ circuit presented in this paper exploits the use of current mode ladder structures applied to MOS transistors [5], [6]. A generic MOS ladder structure, configured as current source, is shown in Fig. 3. All transistors are proportional to a unit size ratio W/L by either a factor 1, $N-1$, or $N/(N-1)$. This way, branch currents I_i have an attenuation ratio of N from each branch to the next one. In the ‘Stochastic I-Pot’ circuit, we use two of these ladder structures.

The first ladder structure, with attenuation ratio around $N=10$, selects an operating current range. This range ladder has 6 output branches, so that the output current can be selected between the input reference current I_{REF} and around $I_{REF}/10^6$. In our particular implementation, we set $I_{REF} = 100\mu A$, so that the minimum range current is about 100pA.

For the second ladder structure, we use an attenuation ratio of $N = 2$. This allows for selecting any binary combination of current branches, in the same way a current DAC would do. However, we do not want to have a high precision (like 8 bit) current DAC within each I-Pot, because they would require extremely large transistor sizes and would most probably not provide such precision for very small currents down to pico-amperes.

In our approach we use ladder structures with attenuation ratio $N = 2$, with a large number of branches, but with small transistor sizes so that we intentionally provide large mismatches between the current branches. By having a large number of branches, each with large mismatch, we achieve a good coverage of possible output current combinations. This can be better understood with the help of Fig. 5, where we show measurements for a ladder with input current 300pA, attenuation ratio $N = 2$, and 8 branches. The unit transistor size is

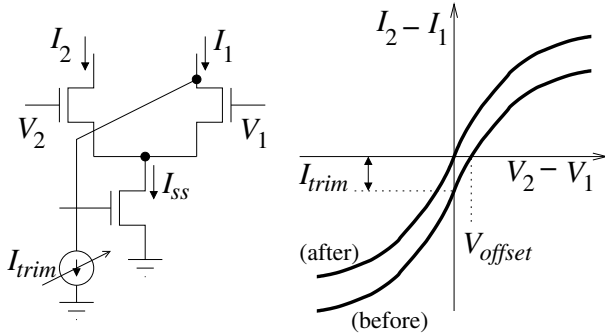


Fig. 2: Illustration of differential pair offset trimming using programmable bias currents

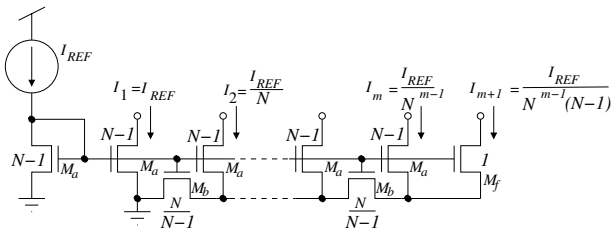


Fig. 3: Schematic of a generic MOS transistor based ladder structure that provides output currents ratioed by factor N .

$W/L = 1/0.7$. For a transistor of this size, fabricated in the AMS 0.35 μm CMOS process [6], [7], and driving a current of 500pA, results in a current mismatch standard deviation of around $\sigma \approx 35\%$, as can be seen by interpolating the measurements shown in Fig. 4. Fig. 5(a) shows the output current obtained as function of the 8-bit digital word w_{val} that controls the combination of branches. As can be seen, this characteristic differs dramatically from a conventional stair-case that a high-precision 8-bit DAC would provide. However, suppose we introduce a look-up table between the digital word we provide and the one physically applied to the ladder structure, so that the output currents become ordered. The result is shown in Fig. 5(b) for the same ladder and bias reference current. Now we see a monotonic increasing dependence between the digital control word w_{ord} and the output current. It does not matter that this relationship is not perfectly linear. Our objective is simply to provide a bias current as close as possible to a desired value. Such objective is limited by the intervals between consecutive current values in Fig. 5(b). To characterize these intervals, we show in Fig. 5(c) the relative difference between the consecutive values in Fig. 5(b),

$$\Delta_{rel} = 2 \left| \frac{I_n - I_{n+1}}{I_n + I_{n+1}} \right| \quad (1)$$

As can be seen, we have errors below 10% for the whole range except the first 1/20 of the range, and below 1% for last 1/4 of the range. But this was a ‘lucky’ particular case. It is perfectly possible to find situations where the mismatch plays against us and we obtain an unfortunate extremely large maximum gap. This is for example, the case illustrated in Fig. 6, for another I-Pot, exactly equal to the one used for Fig. 5. Such situations occur for example, when the maximum branch current I_1 in Fig. 3 results much larger than the sum of all the others. This produces an extremely large gap in the center of the characteristic. In Fig. 6(b) the largest gap was of 92.3pA for a total range of 591.3pA. Consequently, as can be seen in Fig. 6(c), current values in the range between 250 to

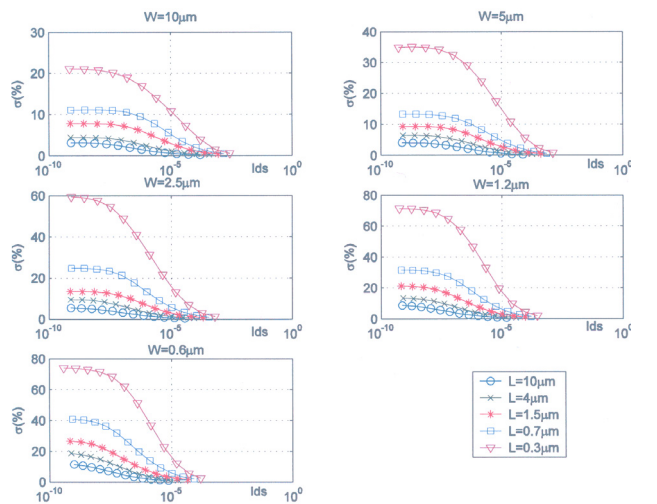


Fig. 4: Current mismatch standard deviation measurements, for NMOS transistors in a 0.35 μm CMOS process. Vertical axes represent standard deviation in %, and horizontal axes represent operating current. Measurements are taken for 30 different transistor sizes, by sweeping width {10, 5, 2.5, 1.2, 0.6} μm and length {10, 4, 1.5, 0.7, 0.3} μm .

350pA cannot be generated with a precision better than 30%.

One can think of several solutions to circumvent this problem. After playing with a few of them and testing them with statistical simulations, we found out that the most reliable solution is to duplicate the output branches of the ladder with attenuation ratio $N = 2$. This not only guarantees there will be no large gaps between consecutive current values, but at the same time reduces dramatically the value of the largest gap found, for the same transistor sizes and input reference current.

Fig. 7 shows the same situation for the circuit in Fig. 6, but where now the output branches are duplicated. Now there are 16 bits to select output branches combinations but the maximum current gap in Fig. 7(b) is now reduced to 0.20pA, excluding the first and last 100pA intervals of the range. The relative error is shown in Fig. 7(c). As can be seen it is less than 0.001 for currents between 137pA and 1214pA. Fig. 8 shows the complete circuit schematics of a ladder with attenuation ratio $N = 2$ and duplicated output branches.

Fig. 9 shows the complete circuit diagram of a stochastic I-Pot cell. Each stochastic I-Pot receives a copy $I_{REFcopy}$ of a common reference current I_{REF} , which is the input to a PMOS $N = 10$ range ladder structure with 6 output branches. The common reference current can be generated by any bandgap type circuit [8] with temperature compensation, or provided off-chip through

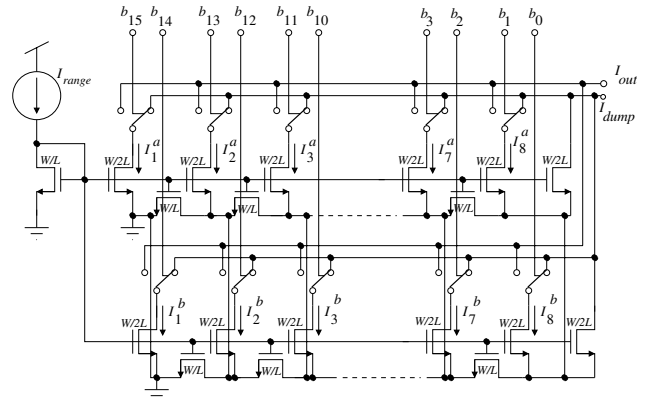


Fig. 8: Circuit schematic of ladder structure with attenuation ratio $N=2$ and duplicated output branches

an extra pin. The digital word w_{range} selects just one of the range ladder outputs (not a combination of them). This current I_{range} sets the coarse mode range of the I-Pot output current. Current I_{range} is now fed to the input of an NMOS $N = 2$ ladder structure with duplicated output branches. Let us call this ladder a “stochastic ladder”. In our particular case we implement 16 (2×8) duplicated branches. The particular combination of output current branches is controlled by the digital word in register w_{val} . The output of this ladder I_a can be optionally sign inverted by transmission gates $sw1 - sw3$, controlled by

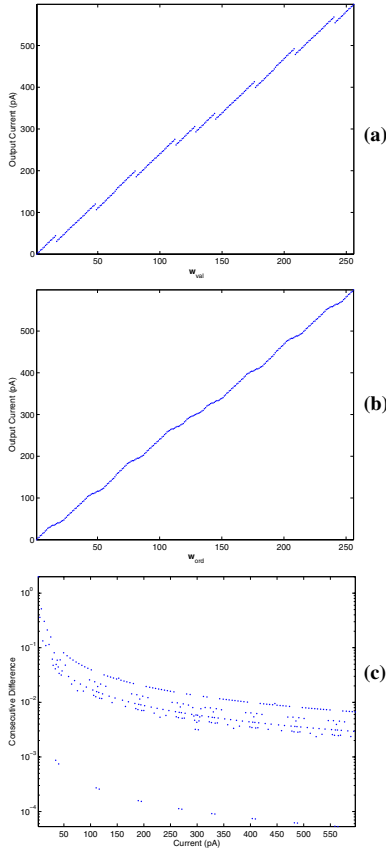


Fig. 5: Illustration of mismatch effects in a MOS ladder structure with ratio factor $N=2$. (a) Output currents versus digital control word, (b) output currents after ordering, (c) relative difference between consecutive values.

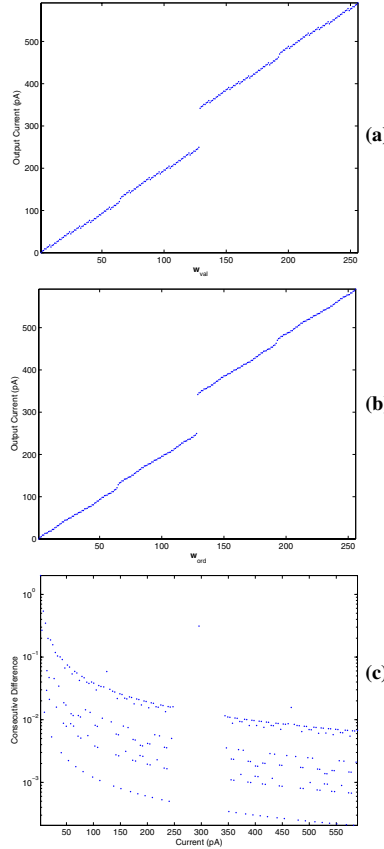


Fig. 6: Illustration of an ‘unlucky’ ladder example. (a) Output currents versus digital control word, (b) output currents after ordering, (c) relative difference between consecutive values.

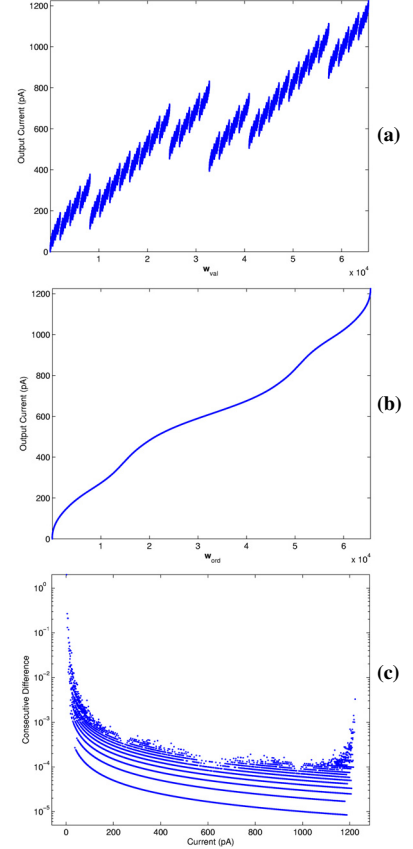


Fig. 7: Illustration of a ladder structure with duplicated output branches. (a) Output currents versus digital control word, (b) output currents after ordering (c) relative difference between consecutive values.

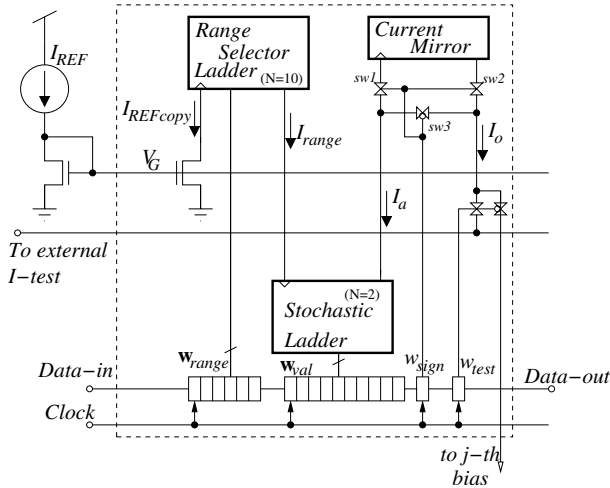


Fig. 9: Circuit diagram of complete I-Pot cell

the state of an extra register w_{sign} , which inserts or not a PMOS current mirror in the output current path. Finally, the signed output current I_o is directed to either its destination bias point, or to a chip output pin I_{test} for characterization purposes, depending on the state of register w_{test} . All registers, w_{range} , w_{val} , w_{sign} and w_{test} are shift registers, connected in series, and clocked by the same clock signal. I-Pot cells can be chained directly in series by chaining their shift registers sharing all the same clock signal. All I-Pot cells share also the same gate line V_G and test line I_{test} .

The main drawback of the present I-Pot approach is that each I-Pot of each fabricated chip needs to be characterized individually. The good news are that this is quite easy to do by using a host computer that loads the chained shift registers, while at the same time we require the use of just one single external current metering instrument.

The procedure for characterizing the I-Pots of a chip is as follows:

1. Each I-Pot has to be characterized individually. Consequently, the w_{test} bit of only one single I-Pot has to be set to ‘active’. All others must be disabled. This way, only one single I-Pot output is connected to external line I_{test} .
2. Sweep the two signs for the active I-Pot.
3. For the selected I-Pot and sign, sweep all current ranges through digital word w_{range} .
4. For the selected w_{range} , sweep all 20 output current branches, measure the selected branch with the external current meter through pin I_{test} , and store it in a file in the computer.

After completing the measurements for one I-Pot, we will have stored in the computer a total of 2 signs \times 6 ranges \times 16 branches = 192 current values. For each sign and range, we can now produce all 2^{16} possible combinations, order them, and find the maximum gap. What now remains to do, is writing a little program that given a desired I-Pot value will return the optimum w_{val} and w_{range} that gives the minimum error.

III. Experimental Results

A set of identical I-Pots was fabricated in the AMS $0.35\mu m$ CMOS process. The stochastic ladder uses 16

duplicated output branches, and the unit transistor of the ladder structure has a size of $W = 1\mu m$, $L = 0.7\mu m$. This ladder was intentionally made with a small unit transistor to increase mismatch, and therefore improve its stochasticity. The range ladder used 6 output branches, and the input current to the range ladder was set to $100\mu A$. The range ladder was designed according to Fig. 3 with an attenuation ratio of $N = 11$, approximately. Transistor sizes for the range ladder were $W = 10\mu m$, $L = 1\mu m$ for transistors M_a , $W = 1\mu m$, $L = 1\mu m$ for transistors M_b , and $W = 1\mu m$, $L = 1\mu m$ for transistor M_f . Note that, according to Fig. 3, we did not use the exact correct sizing for transistors M_b , which should have been instead $W = 1.1\mu m$, $L = 1\mu m$. The consequence of this is simply that the attenuation factor between consecutive range currents will not be equal to 11, but will vary slightly. For us, this is not of critical importance, as long as a certain overlap between consecutive ranges is produced, as will be explained later. The I-Pot schematic, as shown in Fig. 9, includes a 24-bit shift register (6 bits for the range ladder, 16 bits for the stochastic ladder, one sign bit, and one test bit). It turns out that the most area consuming part of the I-Pot are these shift registers. Because of this we used a dynamic shift register. After loading the complete shift register, the data is copied into static latches. The resulting layout size of the fabricated I-Pot is $130\mu m \times 68\mu m$. When we designed this same I-Pot using a conventional static edge-triggered master-slave shift register, the size of its layout was $275\mu m \times 64\mu m$.

After measuring one of the fabricated I-Pots we obtain the currents shown in Fig. 10. Each of the six subgraphs corresponds to one of the available ranges provided by the range ladder. In each subgraph we have added the ordered version of the measured current values. This ordered version is drawn with the continuous line. The minimum and maximum current values provided by each range are as follows. First range $[0.4\mu A, 176\mu A]$, second range $[30nA, 12.7\mu A]$, third range $[1.9nA, 673nA]$, fourth range $[126pA, 44.0nA]$, fifth range $[9.9pA, 3.28nA]$, and sixth

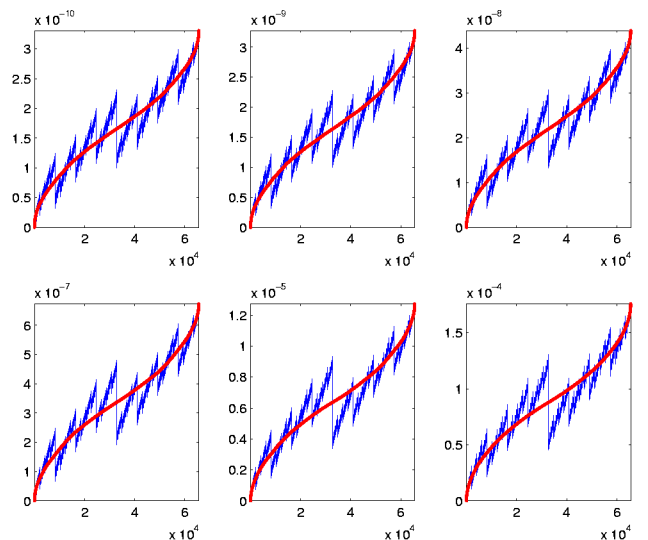


Fig. 10: Measured Currents of one of the fabricated I-Pots for all six current ranges. Continuous lines show the same values after ordering. Vertical axes are measured currents, horizontal axes are index numbers for the $2^{16}=65536$ measurements of each range.

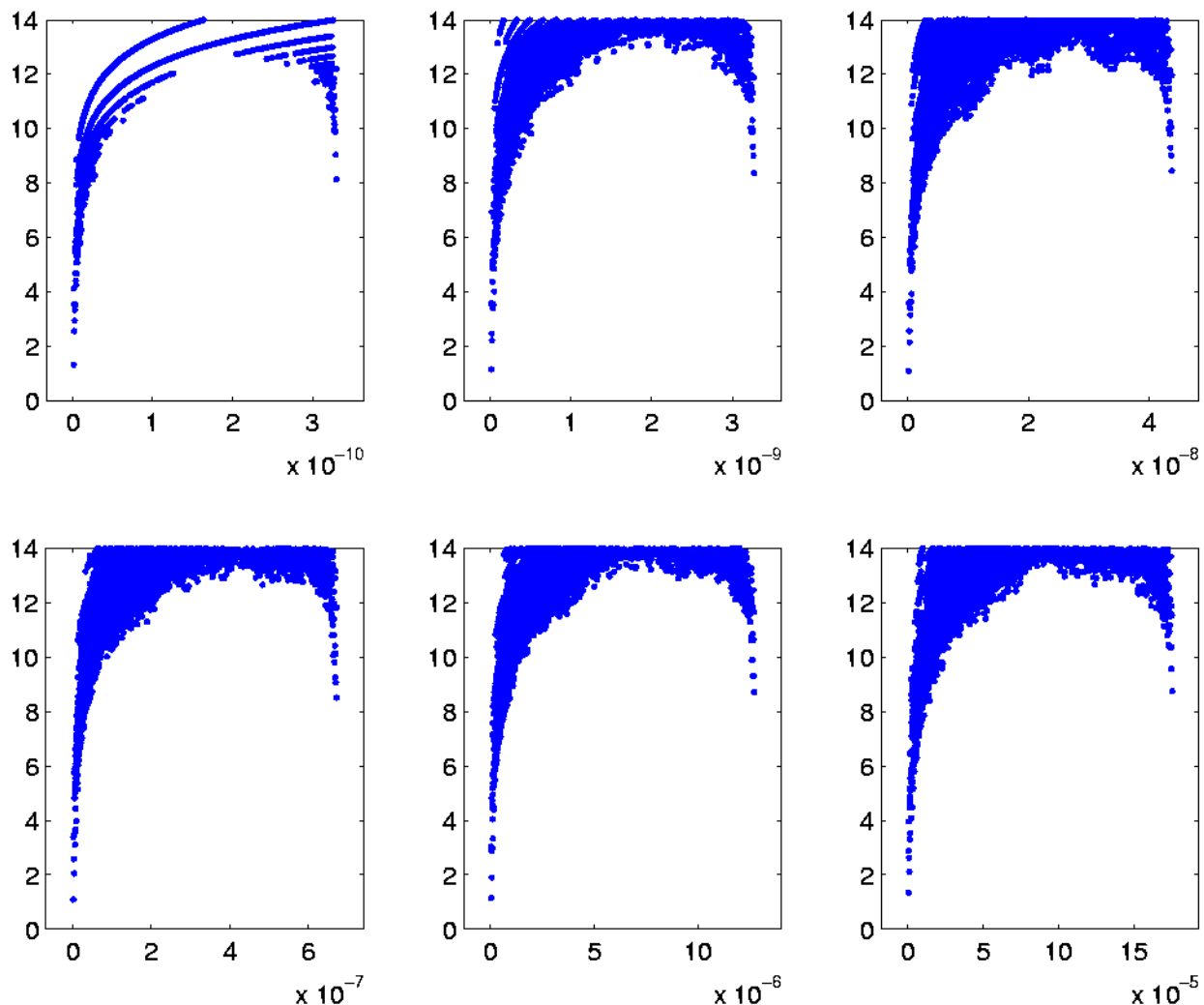


Fig. 11: Computed relative increments between ordered consecutive values (see eq. (1)), expressed in bits. Vertical axes are resulting bits, while horizontal axes are absolute measured currents.

range [1.2pA, 331pA]. With the ordered measured values we can now compute the difference between them, according to eq. (1). Fig. 11 shows these values, expressed in bits¹ as function of currents. Striation effects can be observed, specially as current decreases, due to quantization effects in the data acquisition instrument. We can see that the maximum resolution is obtained for the central parts of the ranges, reaching values as high as 13-bits. On the other hand, for the external parts of the ranges the resolution decreases dramatically down to values as low as 1-bit. This is because in the central part of the ranges there is a higher density of redundant values than on the extremes of the ranges. However, if the ranges overlap, we can increase the density of redundant values and improve the resolution. The procedure is as follows. Let us take all the measured values of all six ranges and order them as one unique set of current values. Each current value is uniquely defined by its range and its 16 bit word within that range. Let us now compute the difference of consecutive values, as defined by eq. (1), and express them in bits. The result is shown in Fig. 12. We can still see very well the regions of the six ranges with

their respective maximum resolution central parts of up to 13-bits. However, the resolution of the extreme regions of the ranges has improved to values of above 8-bits. Neglecting the two extreme regions of the whole merged six ranges, the worst resolution is obtained for currents around 0.7μA, yielding a resolution of 8.05-bits. The first current value showing a resolution above 8 bits is 19.6pA, and the largest one 176μA.

IV. Conclusions

A compact, versatile and powerful circuit for generating digitally controlled precise bias currents is presented. 8-bit precision has been verified from currents as low as 19.6pA up to values of 176μA (almost 7 decades). This circuit is specially handy for experimenting with current-mode circuits operating in weak inversion, where mismatch is high and operating range extends over several decades. It is also very useful for experimenting with new circuits, where it might be desirable to include a large number of (fine-)tunable current biases for trimming gains and offsets. The only drawback is that each I-pot needs to be characterized individually using an external off-chip current metering instrument. If the precise current value of the I-pot is not of critical importance, but the user only needs to know the ordered sequence of the digitally controlled values, the external current meter is not

1. $\frac{1}{2^{n_{bits}}} = \Delta_{rel} \Leftrightarrow n_{bits} = -\log_2(\Delta_{rel}) = -\frac{\ln \Delta_{rel}}{\ln 2}$

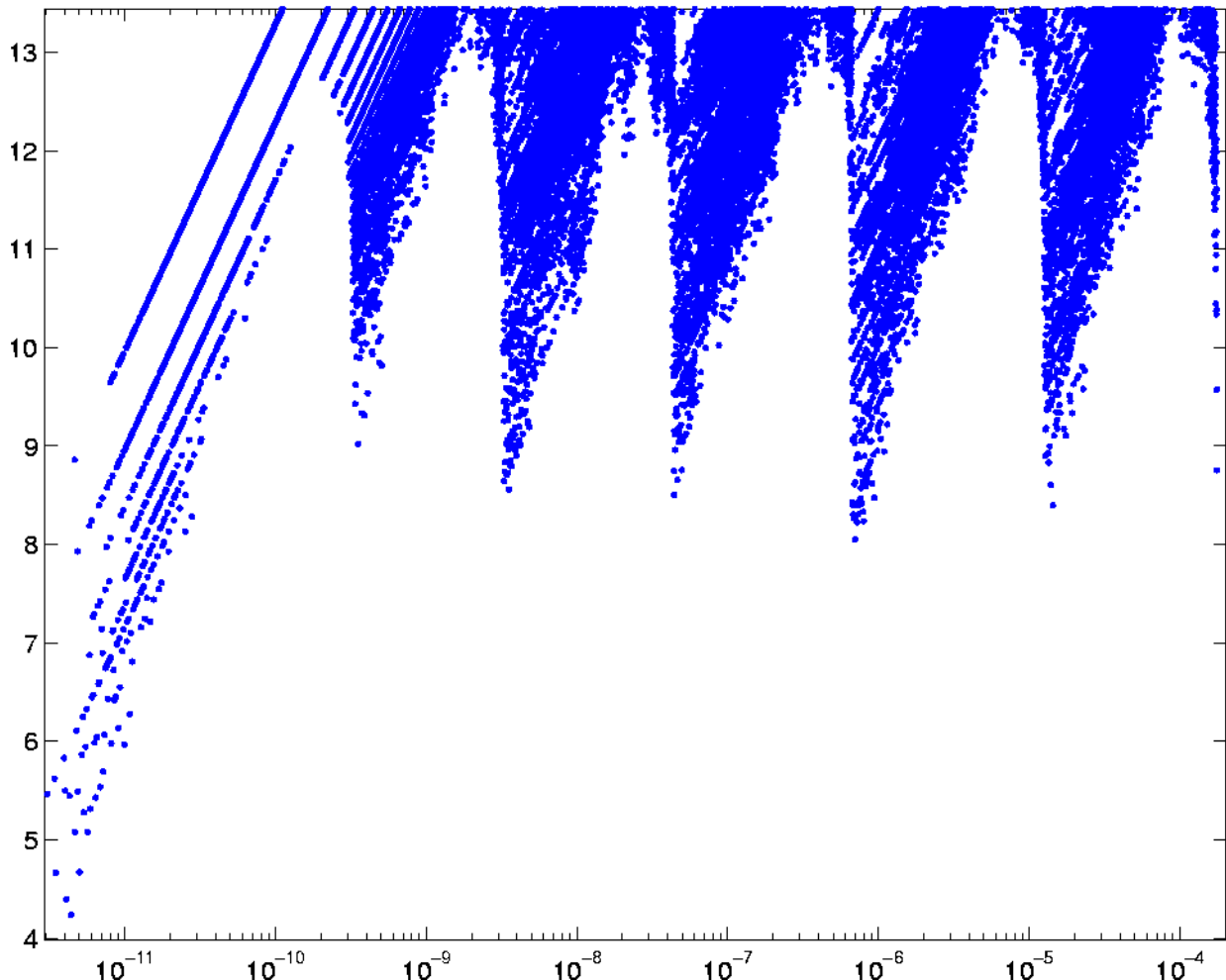


Fig. 12: Computed relative increments, expressed in bits, when considering all measured values of all six ranges as a unique set. Vertical axis represents resulting bits, while horizontal axis represents absolute measured current.

necessary. Instead, one can include an on-chip current-to-frequency circuit (oscillator) and monitor the frequency.

V. Acknowledgements

This work was partially supported by spanish grants TIC2002-10878-E, TIC-2003-08164-C03-01 (Samanta), TEC-2006-11730-C03-01 (Samanta2) and EU grant IST-2001-34124 (Caviar).

VI. References

- [1] C. A. Laber, C. F. Rahim, S. F. Dreyer, G. T. Uehara, P. T. Kwok, and P. R. Gray, "Design Considerations for a high-Performance 3 μ m CMOS Analog Standard-Cell Library," *IEEE J. Solid-State Circuits*, vol. SC-22, No. 2, pp. 181-189, April 1987.
- [2] T. Delbrück and A. Van Shaik, "Bias Current Generators with Wide Dynamic Range," *Int. Journal of Analog Integrated Circuits and Signal Processing*, No. 43, pp. 247-268, June 2005.
- [3] R. R. Harrison, J.A. Bragg, P. Hasler, B.A. Minch, and S.P. DeWeerth, "A CMOS programmable analog memory-cell array using floating-gate circuits," *IEEE Trans. on Circuits and Systems, Part II*, vol. 48, No. 1, pp. 4-11, Jan. 2001.
- [4] R. L. Geiger and E. Sánchez-Sinencio, "Active Filter Design Using Operational Transconductance Amplifiers; A Tutorial," *IEEE Circuits and Devices Magazine*, vol. 1, pp. 20-32, March 1985.
- [5] K. Bult and G.J.G.M. Geelen, "An inherently linear and compact MOST-only current division technique," *IEEE J. Solid-State Circuits*, vol. 27, No. 12, pp. 1730-1735, Dec. 1992.
- [6] B. Linares-Barranco, T. Serrano-Gotarredona, and R. Serrano-Gotarredona, "Compact Low-Power Calibration Mini-DACs for Neural Massive Arrays with Programmable Weights," *IEEE Trans. on Neural Networks*, vol. 14, No. 5, pp. 1207-1216, September 2003.
- [7] T. Serrano-Gotarredona and B. Linares-Barranco, "CMOS Mismatch Model valid from Weak to Strong Inversion", *Proc. of the 2003 European Solid State Circuits Conference, (ESSCIRC'03)*, pp. 627-630, September 2003.
- [8] P.R. Gray, P.J. Hurst, S.H. Lewis, and R. G. Meyer, *Analysis and Design of Analog Integrated Circuits*, 4th Edition, John Wiley, 2001.